phenyl and 50% polysiloxane) 10 m × 0.53 mm wide bore column. UV spectra were recorded on either a Hewlett-Packard 8415A single-beam photodiode array or a Perkin-Elmer 452 double-beam spectrophotometer. Mass spectra were recorded on a Kratos MS-30 double-focusing dual-beam spectrometer at 20 eV ionizing voltage.

Materials. **1a** and **1b** were synthesized according to a previously reported procedure via a Grignard reaction starting with either *trans*-4-pentyl(4-cyanophenyl)cyclohexane (Merck Licristal/ZLI-114) for **1a** or *trans*-4-heptyl(4-cyanophenyl)cyclohexane (Merck Licristal/ZLI-115) for **1b** and 1-bromobutane (Aldrich, 99%). Both ketones were more than 99% pure as determined by GLPC after recrystallizations from ethanol.

trans- and *cis*-**3a** and **2a** were obtained from a solution of 300 mg of **1a** in benzene (Baker reagent) that had been purged with nitrogen for 5 min and irradiated to nearly 100% conversion. The photoproducts were separated on a silica (Baker, 60-200 mesh) column with 97/3 (v/v) hexane–ethyl acetate (Aldrich reagents) as mobile phase. *trans*-**3a** and **2a** were characterized by their ^{1}H and ^{13}C NMR spectra, mass spectra, and co-injection with irradiated samples of **1a** whose photoproduct retention times had been previously determined. *cis*-**3a** was identified by its proton NMR spectrum. Both diastereomeric cyclobutanols have characteristic cyclobutyl proton resonances in the 1.8–2.8-ppm region.[30] The ^{1}H spectrum of the trans isomer differs from that of the cis in the location of the doublet resonance corresponding to the protons of the methyl group on the cyclobutyl ring. For the cis isomer, the doublet resonated at 0.62 ppm (J = 6.9 Hz) while for the trans isomer it was found at 1.1 ppm (J = 6.9 Hz). The ^{13}C spectrum of the trans isomer showed a peak at 78.4 ppm characteristic of tertiary carbons bearing a hydroxyl group and its mass spectrum exhibited an m/e peak at 314, as well as M − 18 and M − 28 peaks characteristic of 1-phenylcyclobutanols.[30] On the silica chromatographic column, the cis isomer eluted after the trans.

2a has a melting point of 62.0–65.0 °C. NMR spectrum: 7.88 (d, J = 8.25 Hz, 2 H, aromatic), 7.25 (d, 8.25 Hz, 2 H, aromatic), 2.58 (s, 3 H, methyl α to carbonyl), 2.56 (m, 1 H, cyclohexyl α to phenyl group), 1.89 (d, 4–5 H, cyclohexyl), 1.2–1.1 (m, alkyl and cyclohexyl), 0.9 (t, 3 H, terminal methyl). The mass spectrum of **2a** exhibits an m/e peat at 272, its expected molecular ion.

2b was synthesized according to the same procedure used to obtain **1**, except methyl iodide (Fisher reagent) instead of 1-bromobutane was employed to form the Grignard reagent. **2b** exhibited mp 62.8–64.8 °C and a proton NMR spectrum almost identical to that of **2a**. The mass spectrum of **2b** displayed an m/e peak at 300, its expected molecular ion.

Treatment of either homologue of **1** with deuterium oxide (MSD Isotopes, 99% *d*) and Na_2CO_3 in monoglyme[31] (Aldrich, anhydrous, 99%) yielded ketone with >90% deuterium at the position α to the carbonyl group as determined from comparisons of the ^{1}H integrals of the α methylene resonances (2.9 ppm) from treated and untreated **1**.

Irradiation Procedures. Irradiations were performed with a Hanovia 450 W medium pressure Hg arc lamp. Temperature control was achieved using either a Haake HK-2 or a Forma Scientific circulating water bath. Prior to photolysis, samples were purged with nitrogen for ca. 5 min in their isotropic phases, transferred to (0.8–1.1) × 100 mm capillary tubes, and flame-sealed. Irradiations were performed through water, a Pyrex glass filter, and a Corning 0-51 cutoff (>30% at 380 nm) filter. Irradiations of three samples at each temperature were conducted to less than 10% ketone conversion. The contents of the capillaries were then dissolved in hexane (Aldrich, HPLC grade) and analyzed by gas chromatography. The E/C ratios, uncorrected for detector response, represent an average of triplicate analyses of each of the three samples at each temperature.

Acknowledgment. We thank E. Merck for a generous supply of Licristals ZLI-114 and ZLI-115 and Dr. Jawad Naciri of the Naval Research Laboratory for the use of the Optiphot microscope. The National Science Foundation is gratefully acknowledged for its support of this research.

(30) Wagner, P. J.; Kelso, P. A.; Kemppainen, A. E.; McGrath, J. M.; Schott, H. N.; Zepp, R. G. *J. Am. Chem. Soc.* **1972**, *94*, 7506.

(31) Trost, B. M.; House, H. O. *J. Org. Chem.* **1965**, *30*, 1341.

Mixed-Valence, Conjugated Quinone and Imide Anion Radicals. An ESR Investigation

Stanton F. Rak and Larry L. Miller*

Contribution from the Department of Chemistry, University of Minnesota, Minneapolis, Minnesota 55455. *Received August 8, 1991. Revised Manuscript Received October 11, 1991*

Abstract: Anion radicals of linear polyacene diquinones and diimides were produced electrochemically and studied by ESR. The odd electron of substituted 1,4,8,11-pentacenetetrone anion radicals is localized (in a naphthoquinoid unit) and hops from one quinone to the other. The hopping rate was measured. The anion radicals of similarly sized anthracenetetracarboxylic acid 2,3:6,7-diimides have a delocalized odd electron, and there is relatively high electron density on the bridge. The results are compared to other unconjugated two-electrophore anion radicals.

Recent studies in our laboratories have been directed toward the synthesis and properties of linear, rigid polyacene quinones and imides.[1-5] These molecules were designed to have long delocalization lengths and more than one quinone or imide electrophore. These structural features led us to examine the optical and electrical properties of the anion radicals, which displayed unusual properties, indeed, including near-infrared (near-IR) absorption bands at wavelengths as long as 2000 nm[1-3] and electrical conductivities as high as 1 S cm^{-1}.[4] It was proposed that a central structural issue was the delocalization or localization of the unpaired electron. Based on cyclic voltammetry (CV), near-IR, IR, and ESR spectra, and molecular orbital (MO) calculations, anion radicals containing one aryl ring between the electrophore groups, e.g., **1**$^-$ and **4**$^-$, were classified as delocalized.[1,2] Anion radicals having naphthalene or anthracene bridges connecting quinone electrophores, i.e., **2**$^-$ and **3a**$^-$, gave very different optical spectra, and based upon MO calculations, it was suggested that the unpaired electron in these anion radicals was localized on one quinone unit at any instant.[3] As such, the anion radicals could be considered mixed-valence species.

π-Electron localization was unexpected because the two electrophores of **2**$^-$ and **3a**$^-$ are formally part of a planar, conjugated π-system. In the present study ESR was used to examine this

(1) Rak, S. F.; Jozefiak, T. H.; Miller, L. L. *J. Org. Chem.* **1990**, *55*, 4794.
(2) Almlöf, J.; Jozefiak, T. H.; Feyereisen, M. W.; Miller, L. L. *J. Am. Chem. Soc.* **1990**, *112*, 1206.
(3) Almlöf, J.; Jozefiak, T. H.; Feyereisen, M. W.; Miller, L. L. *J. Am. Chem. Soc.* **1989**, *111*, 4105.
(4) Forkner, M. W.; Miller, L. L.; Rak, S. F. *Synth. Met.* **1990**, *36*, 65.
(5) Christopfel, W. C.; Miller, L. L. *J. Org. Chem.* **1986**, *51*, 4169. Kenney, P. W.; Miller, L. L. *J. Chem. Soc., Chem. Commun.* **1988**, 85. Thomas, A. D.; Miller, L. L. *J. Org. Chem.* **1986**, *51*, 4160.

0002-7863/92/1514-1388$03.00/0

speculative hypothesis and provide definitive evidence for localization in the quinone anion radicals of the type 3^-. In contrast, the very similar imide anion radicals of type 5^- are shown to be delocalized. The rates of intramolecular electron hopping are reported for $3b^-$ and $3c^-$ and compared to the rates for the unconjugated triptycene derivative 6^- and other anion radicals.

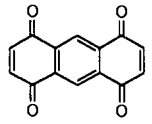

1

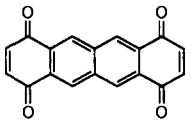

2

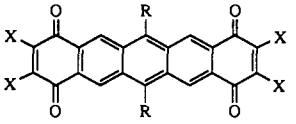

3a R = H, X = H
3b R = H, X = CH_3
3c R = 1-hexyl, X = CH_3

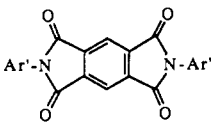

4

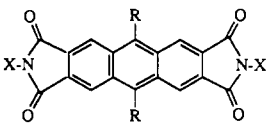

5a R = H, X = Ar'
5b R = OMe, X = Ar'
5c R = OMe, X = Ar

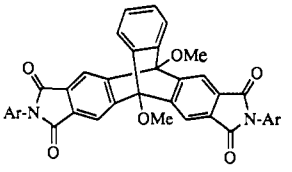

6

Ar = 4-tert-butylphenyl
Ar' = 2,5-di-tertbutylphenyl

Results and Discussion

Synthesis. Anthracene-bridged dielectrophores were chosen for study, in part because they were synthetically accessible. The specific examples were chosen to be more soluble and have better anion-radical stability than previously reported for **3a**. Compounds **3b,c** were prepared from the precursors **7b,c** developed by Hart[6] and Schlüter,[7] respectively. The process can be understood in

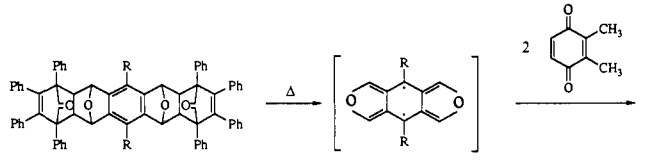

7b R = H
7c R = 1-hexyl

8

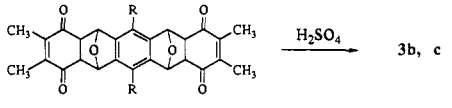

3b, c

terms of two retro-Diels–Alder reactions to give the hypothetical **8** followed by two Diels–Alder additions with 2,3-dimethylbenzoquinone to give dioxo adducts. These adducts are then dehydrated with sulfuric acid.

Compound **3b** had only limited solubility in common organic solvents, but the dihexyl-substituted **3c** dissolved readily in CH_2Cl_2, $CHCl_3$, or DMF. The orange/red color of **3c** in CH_2Cl_2 or $CHCl_3$ solution dissipated readily in the presence of room light and air to give pale yellow solutions. The product isolated from those solutions was **9**, where oxygen is added across the center ring to

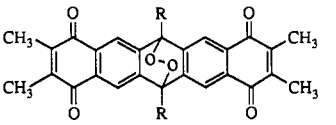

9 R = 1-hexyl

give the *endo*-peroxide. This reaction, similar to that studied for **5c**,[1] is a photooxidation, and thus, **3c** was handled with minimum exposure to light. **3b** was stable in the presence of room light and air.

6 was synthesized by addition of benzyne to the center ring of dimethoxyanthracene diimide **5c**.

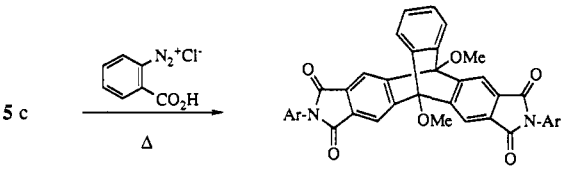

Cyclic Voltammetry. In general, the voltammograms were recorded in DMF containing 0.1 M Bu_4NBF_4. The working electrode was a glassy carbon disk, and ferrocene was added as an internal standard for the saturated calomel electrode (SCE) reference. The apparent $E°$ was taken as the midpoint between the anodic and cathodic peak potentials. The anodic–cathodic peak separations were 60 ± 5 mV except for **3c** which gave 80 mV. The relative anodic/cathodic peak currents were approximately equal, and the peak potentials were independent of scan rate, indicating that the $E°$ values (Table I) represent a thermodynamic equilibrium.

It has been previously reported that **3a** reduces in DMF with apparent $E° = -0.72$ and -0.84 V.[3] Because this compound was so insoluble, it was difficult to get good cyclic voltammograms. Compound **3b** was similar. One of the more simple voltammograms was determined using DMF, 0.1 M $LiClO_4$. It showed two poorly resolved reduction peaks at $E° = -0.79$ and -0.94 V. In an attempt to begin with soluble material, bulk electrolysis generated solutions of the anion radical $3b^-$ which was then studied (Figure 1). Complex surface electrochemistry is revealed here and in voltammograms obtained in other solvents and with other electrode materials, which is related to the adsorption of the neutral, but it was not completely unraveled and it will not be discussed.

The voltammogram of **3c** is shown in Figure 2. The hexyl groups aid in solubilizing the diquinone and allowed for its examination in CH_2Cl_2, 0.1 M nBu_4NBF_4. Two closely spaced, but distinct, redox couples were present at $E° = -0.83$ and -0.98 V.

Table I. Reduction Potentials[a]

compd	$-E°'$ (V, SCE)	
1[b]	0.26	0.74
2[b]	0.50	0.75
3a[b]	0.72	0.84
3b[c]	(0.79)	(0.94)
3c[d]	0.83	0.98
4[e]	0.71	1.43
5a[e]	1.07	1.53
5b[e]	1.03	1.52
5c[e]	1.01	1.45
6	1.23	1.39
10[b]	0.30	0.53

[a] Measured in DMF, 0.1 M nBu_4NBF_4, scan rate 150 mV/s, glassy carbon working electrode, SCE reference. $E°' = (E_p^a + E_p^c)/2$. The values are reproducible within ±10 mV. [b] Reference 3. [c] Recorded in 0.1 M $LiClO_4$/DMF; values are cathodic peak potentials. [d] Recorded in 0.1 M nBu_4NBF_4/CH_2Cl_2, scan rate 50 mV/s. ΔE_p(anodic–cathodic) = 80 mV. [e] Reference 1.

(6) Luo, J.; Hart, H. *J. Org. Chem.* **1988**, *53*, 1341.
(7) Schlüter, A.-D.; Blatter, K. *Macromolecules* **1989**, *22*, 3506.

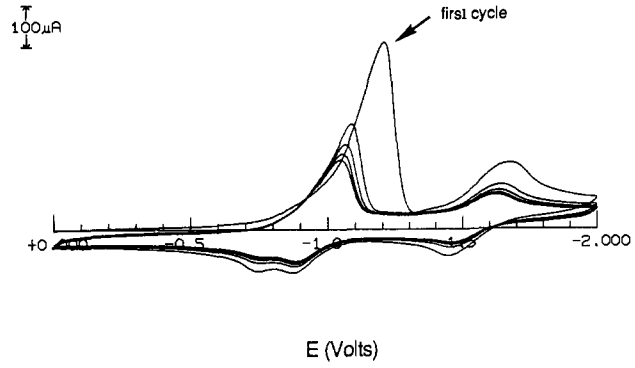

Figure 1. CV of $3b^-$ in DMF, 0.1 M Bu_4NBF_4 (sweep rate 1.0 V s^{-1}, starting potential 0.0 V).

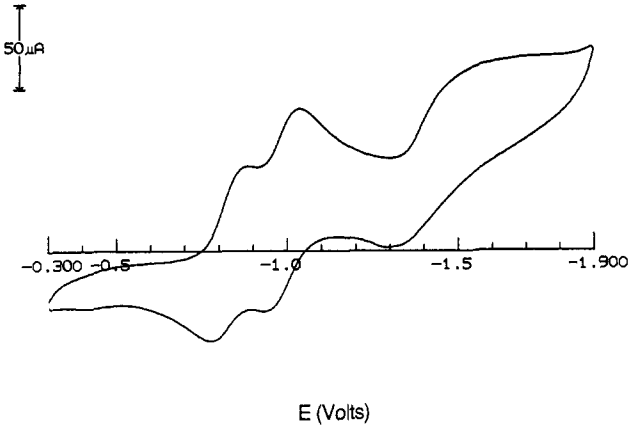

Figure 2. CV of **3c** in CH_2Cl_2, 0.1 M Bu_4NBF_4 (sweep rate 200 mV s^{-1}).

A third, kinetically irreversible peak was present at −1.5 V. No change in the voltammogram was observed during repetitive cycling between −0.3 and −1.2 V.

The reduction potentials of the diquinone series make for an interesting comparison. As expected from the electrochemistry of monoquinones,[1,2,8] the anthracene diquinone **1** was the easiest to reduce followed by the tetracene diquinone **2**[3] and the pentacene diquinones. A similar trend was observed for the second reduction processes. The $\Delta E°$ values between the first and second reduction couples were 0.48 V for **1**, 0.25 V for **2**, and 0.15 V for **3b** and **3c**. One explanation for the smaller $\Delta E°$ for longer molecules is that repulsions in the dianion are diminished as the aryl bridge is extended.

Likewise for the diimides, the first reduction of the pyromellitic diimide derivative **4** (−0.71 V) occurs at a more positive potential than for the anthracene diimide derivatives **5a** (−1.07 V), **5b** (−1.03 V), and **5c** (−1.01 V). However, the $\Delta E°$ values for the **5** series were large (0.41–0.49 V) in comparison to the pentacene diquinones. This may imply greater Coulombic repulsions in the diimide dianions than in the diquinone dianions.

CV on the triptycene bis(phthalimide) **6** showed it to be similar to that of the analogous diquinone **10**.[9] The first reduction of

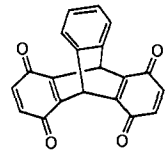

10

6 occurred at −1.23 V, midway between the reduction of anthracene diimide **5c** (−1.01 V) and *N*-phenylphthalmide (−1.36 V). The second reduction of **6** took place at −1.39 V, only 0.16 V more negative of the first reduction. This $E°$ is slightly positive of the second $E°$ for **5c** and considerably positive of that for *N*-phenylphthalimide (−2.22 V). It seems clear that the two electrophores of **6** each take up one electron and the Coulombic repulsions are small.

(8) Jozefiak, T. H. Ph.D. Thesis, University of Minnesota, 1989.

Table II. ESR Coupling Constants[a]

compd	solvent	*a* (G)
$3b^-$	DMF	1.34 (12 H)
$3c^-$	DMF	1.34 (12 H)
$3c^-$	DMF (195 K)	2.89 (6 H)
$3c^-$	CH_2Cl_2	0.20 (4 H), 1.34 (12 H)
$3c^-$	CH_2Cl_2 (185 K)	0.64 (2 H), 2.84 (6 H)
4^-	DMF	0.65 (2 H), 1.17 (2 N)
$5a^-$	DMF	4.24 (2 H), 3.07 (4 H) 0.76 (2 N) 4.12 (2 H),[b] 2.31 (4 H)[b]
$5b^-$	DMF	3.19 (4 H), 0.75 (2 N)
$5c^-$	DMF	3.19 (4 H), 0.68 (2 N)
6^-	DMF	1.16 (2 N)
6^-	CH_2Cl_2	1.19 (2 N)

[a] Spectra recorded in 0.1 M Bu_4BF_4 solutions at T = 294 K unless otherwise noted. Only coupling constants for fully resolved peaks are listed. [b] Calculated values from the McConnell equation, $a_H = Q\rho$, where Q = 23 G. The spin densities, ρ, were determined from a PPP-MO calculation using the b_{2u} SOMO coefficients (symmetry determined with the molecule positioned in the x–z plane).

The most revealing comparison is between the polyacene and triptycene analogues. The differences between the first and second $E°$ values for compounds **3** and **10** are quite similar. Since **10** has been shown to be localized,[9] compounds **3** may be similarly localized. In contrast, comparison of compounds **5** and **6** shows that the first $E°$ values for **5** are more positive and the $\Delta E°$ values for compounds **5** are larger than that for **6**. This can be understood if **6** forms localized ions, but **5** forms delocalized ions (see below). Delocalization makes it easier to add one electron forming 5^-, but since the second electron is in a similar space, the electron repulsion in the dianion 5^{2-} is larger.

ESR Spectra. Potentiostatic electrochemical reductions were performed in situ in the spectrometer cavity because some of the anion radicals were of limited stability or had closely spaced couples. It was found that resolution could be improved if the Pt electrode was pulled up out of the cavity after generation of the anion radical. The initial concentration of the electroactive species ranged from 0.1 and 1.0 mM, the solvent was DMF or CH_2Cl_2, and the electrolyte was 0.05–0.50 M Bu_4NBF_4.

Recall that the odd electron of 1^- is delocalized.[3] It has been contrastingly demonstrated using variable-temperature ESR studies that the odd electron of the unconjugated 10^- is localized.[9] A main objective of the present investigation was to examine the hypothesis that the odd electron of 3^- is also localized.

Electron Localization and Hopping in 3^-. At room temperature in DMF, 0.1 M Bu_4NBF_4, $3b^-$ and $3c^-$ gave identical 13-line ESR spectra with a_H(12 H) = 1.34 G (Table II). In CH_2Cl_2, 0.1 M Bu_4NBF_4, the $3c^-$ spectrum was better resolved, revealing additional splitting on each of the 13 lines; a_H(4 H) = 0.20 G. The couplings are assigned to the 12 methyl hydrogens and the 4 equivalent bridge hydrogens. Thus, at room temperature the odd electron is distributed over both electrophores.

The low-temperature spectra of $3b^-$ and $3c^-$ unequivocally demonstrate that the odd electron is localized on one quinone unit. Thus, as the temperature is lowered, alternant lines broaden, and at the lowest temperatures, spectra with half the number of proton couplings are observed.[10] Using $3c^-$ in DMF, the 13-line 294 K spectrum changed to 7 lines at 210 K. In CH_2Cl_2 the low-temperature spectrum showed each of the 7 lines split into triplet (Figure 3). The less soluble $3b^-$ could only be studied in DMF. In that solvent, the spectra were not completely isotropic and the

(9) Russell, G. A.; Saleman, N. K.; Iwamura, H.; Webster, O. W. *J. Am. Chem. Soc.* **1981**, *103*, 1560.

(10) Freed, J. H.; Fraenkel, G. K. *J. Phys. Chem.* **1962**, *37*, 1156. Wertz, J. E.; Bolton, J. R. *Electron Spin Resonance-Elementary Theory and Pratical Applications*; Chapman and Hall: New York, 1986; p 208.

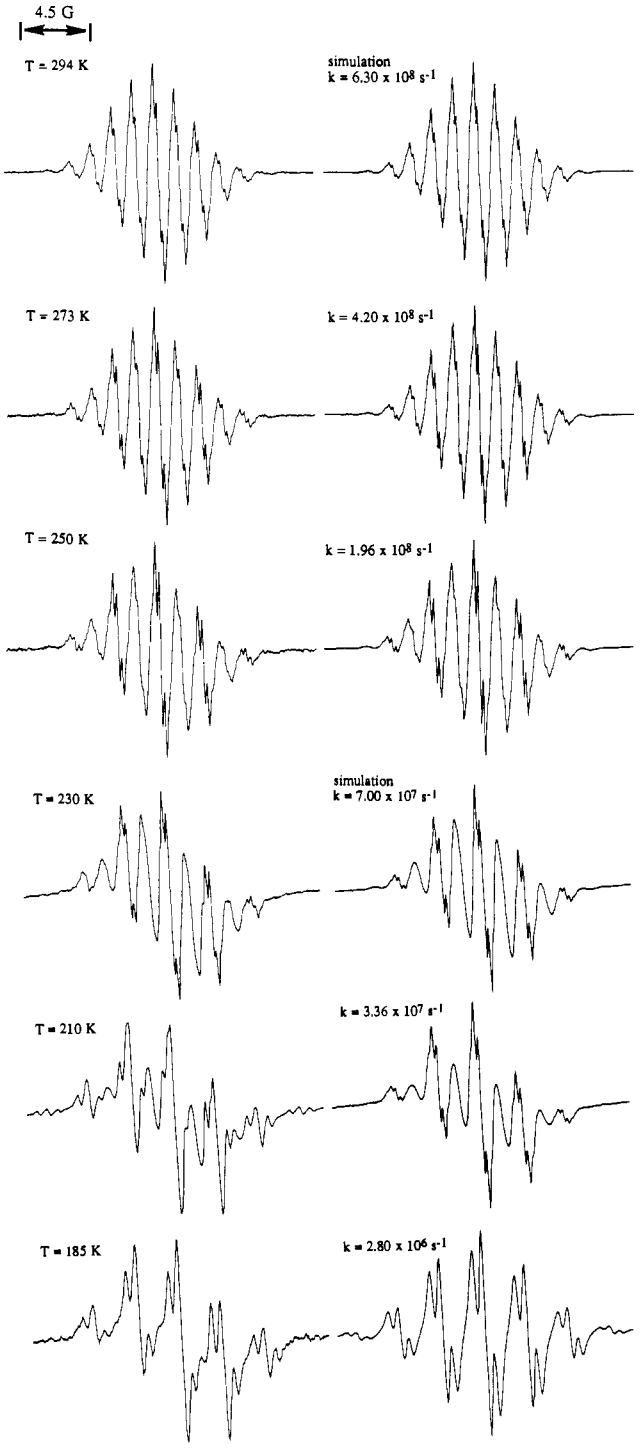

Figure 3. Experimental and simulated ESR spectra of $3c^-$ in CH_2Cl_2, 0.05 M Bu_4NBF_4, at various temperatures.

seven line spectrum was only partially resolved at low temperature (Figure 4). It is noted that at these low temperatures the solvents are rather viscous and anisotropy is quite possible. Also important is the decrease in polarity of the solvent at low temperature. This can affect a_H values and can lead to increased ion pairing or aggregation of the sparingly soluble $3b^-$.

The results lead to a model for 3^- that has a double minimum on the potential energy surface so that the electron is localized on one quinone or the other at any instant. The low-temperature $a_H(6\ H) = 2.84$ and $a_H(2\ H) = 0.64$ G show that each of the localized orbitals of 3^- is similar in electron distribution to the half-filled orbital of 2,3-dimethyl-1,4-naphthoquinone anion radical, which has $a_H(6\ H) = 2.51$ and $a_H(2\ H) = 0.32$ G for the appropriate hydrogens.[11] Both 3^- and dimethylnaphthoquinone

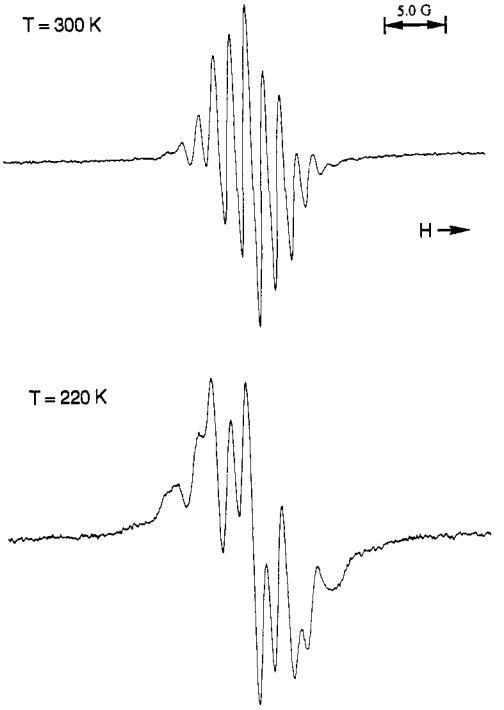

Figure 4. ESR spectra of $3b^-$ in DMF, 0.1 M Bu_4NBF_4, at 300 and 220 K.

Table III. Kinetic Data[a]

anion radical	conditions	$\Delta G^{\ddagger}_{298}$ (kcal/mol)	$\Delta H^{\ddagger}$ (kcal/mol)	$\Delta S^{\ddagger}$ (eu)
$3b^-$	0.1 M Bu_4NBF_4/DMF	6.6		
$3c^-$	0.1 M Bu_4NBF_4/DMF (230 → 200 K)	5.2	4.2	−3
$3c^-$	0.05 M Bu_4NBF_4/CH_2Cl_2	5.4	4.0	−5
$3c^-$	0.50 M Bu_4NBF_4/CH_2Cl_2 (273 → 210 K)	5.3	4.6	−3
6^-	0.1 M Bu_4NBF_4/DMF (340 → 210 K)	6.2	4.1	−7
6^-	0.05 M Bu_4NBF_4/CH_2Cl_2 (294 → 230 K)	6.1	4.5	−5
10^{-}[b]	CH_3CN (298 → 248 K)	8.3	6.2	−7

[a] From variable-temperature ESR measurements. The error in $\Delta G^{\ddagger}$ and $\Delta H^{\ddagger}$ is estimated to be ±20% and in $\Delta S^{\ddagger}$ ±40%. [b] Reference 9.

anion radicals have equivalent methyl groups, indicating that on the ESR time scale the electron is delocalized over both carbonyl groups of one quinone. In this regard, consider an alternative structure for 3^- which involves a "top-to-bottom" instead of "side-to-side" exchange. The localized SOMO would encompass not the 1,4-carbonyl groups but the 1,11-carbonyl groups. The electron would then jump to the 4,8-dicarbonyl conjugated system. Since under these conditions neither monosemiquinones nor 1^- exhibits localization, it seems unlikely that this possibility is realized. Clearly the distance between the quinone groups (and perhaps the polarizability of the long bridge) is important to achieving localization in the absence of strong ion pairing.

The dynamics of the exchange processes were simulated (see Figure 3 for an example), and rate constants for electron hopping were computed at several temperatures. A two-site, intramolecular exchange with no change in structure or ion pairing as the temperature changed was assumed. These data were then used for Eyring plots, leading to the results shown in Table III. The activation parameters for $3c^-$ were the same within experimental error in either DMF or CH_2Cl_2 solvent and were unchanged when measured using the electrode in the cavity or out.[12] The simu-

(11) Rieke, R. D.; Rich, W. E. *J. Am. Chem. Soc.* **1970**, *92*, 7349.

(12) Using $3c^-$ in CH_2Cl_2, cooling to 185 K, and then reheating did not give the original 294 K spectrum. Cooling to 210 K and reheating did give the 294 K spectrum. We speculate that precipitation occurs at 185 K.

lations for $3b^-$ led to a linear Eyring plot over the range 300–230 K, but because the low-temperature spectra were distorted and could not be simulated, there was considerable experimental uncertainty in the analysis and only $\Delta G^{\ddagger}$ is reported.

The absence of an appreciable solvent effect on the rate of electron exchange for $3c^-$ made it of special interest to study the possible effects of ion pairing by changing the bulky Bu_4N^+ to Li^+. Using $3b^-$ in DMF, 0.1 M $LiClO_4$, a distorted 7-line spectrum was observed at room temperature, which closely resembled the low-temperature spectrum found when Bu_4N^+ was used. The use of HMPA solvent (an effective Li^+ ligand) led to the 13-line spectrum observed with Bu_4N^+ at high temperature. It is thus clear that Li^+ ion pairing leads to strong localization at room temperature and that HMPA solvates the cation and increases the rate of electron exchange.

To examine further cation effects, $3c^-$ was studied using 0.05 and 0.5 M Bu_4NBF_4 in CH_2Cl_2. The two Bu_4N^+ concentrations gave the same rate and activation parameters within experimental error. If the anion radical is not ion paired with the bulky Bu_4N^+ and the electron just jumps from end to end, independence of the rate on cation concentration is expected. If the anion radical is ion paired and there is an *intramolecular* jump of the Bu_4N^+ along with the electron, the experimental result is also rational. Ruled out is the mechanism in which an ion-paired species, $3c^-$, Bu_4N^+, dissociates to free ions; the electron jumps in the rate-limiting step, and then a new ion pair forms on the other end. This process would be slower at higher Bu_4N^+ concentration.

Consider the situation more carefully assuming that free ion radicals are present. It is expected that the quinone unit which holds the odd electron in an antibonding orbital would have an expanded molecular framework compared to its counterpart on the other end. Solvent organization should also be different for the ionic and neutral ends of the mixed-valence ion. Electron transfer then involves changes in the nuclear positions of the radical anion and the solvent, and this accounts for the activation energy.

The solvent effect on the reaction rate for $3c^-$ can be modeled in a simple way using an equation suggested by Marcus.[13]

$$4\Delta G_s^{\ddagger} = \lambda_s = e\left(\frac{1}{2r_a} + \frac{1}{2r_b} - \frac{1}{r_{ab}}\right)\left(\frac{1}{D_{op}} - \frac{1}{D}\right)$$

Here, λ_s is the solvent reorganization energy for a thermoneutral reaction, r_a and r_b are the radii of the two reaction centers, r_{ab} is the distance between the centers, D is the dielectric constant, and D_{op} is the refractive index squared. Assuming that $r_a = r_b = 5$ Å and $r_{ab} = 7.5$ Å (center to center) leads to a calculated $\Delta G_s^{\ddagger} = 2.6$ kcal mol^{-1} in DMF and $\Delta G_s^{\ddagger} = 2.2$ kcal mol^{-1} in CH_2Cl_2. These values are smaller in magnitude than the experimental $\Delta G^{\ddagger}$ (which includes internal reorganizations), and the difference between them is less than the experimental error of the ESR measurements. Therefore, the experimental result is not in conflict with the expectations of theory.

It is of interest that the activation parameters for 3^- are quite similar to those previously reported for the triptycene diquinone anion radical 10^- (Table III)[9] and measured for the triptycene diimide anion radical 6^- (see below). This can be interpreted to mean that all three rates are determined by the similar changes in nuclear geometry of the ions and the solvent and a similar distance for electron transfer. The small $\Delta S^{\ddagger}$ values are quite appropriate for a reaction with no change in charge.

Anion radicals which are somewhat less similar, but which have short aliphatic bridges between electrophores, are 11^- and 12^-.

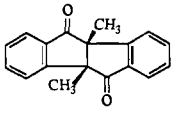

11

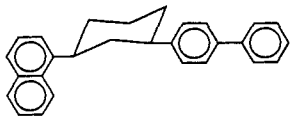

12

In DMF with Bu_4N^+ counterions, 11^- has $k \sim 5 \times 10^8$ s^{-1} at 250 K.[14] Since the naphthyl and biphenyl groups have about the same E°, 12^- also allows an appropriate comparison. Here, $k = 4 \times 10^9$ s^{-1} at room temperature for γ-radiation-generated ions in tetrahydrofuran.[15] Clearly, the exchange rates for anion radicals with short aliphatic bridges are similar to those for 3^- (4.2×10^8 s^{-1} at 273 K). This demonstrates that, for anion radical exchange across short bridges, sp^2 carbons are similar to sp^3 carbons.

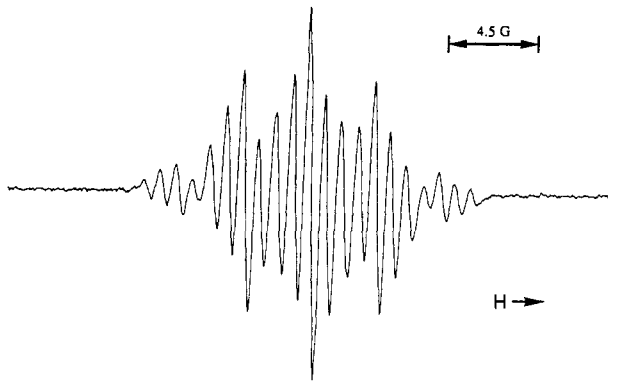

Figure 5. ESR spectrum of $5c^-$ in DMF, 0.1 M Bu_4NBF_4, at 298 K.

Electron Delocalization in 5^-. Although **3** and **5** differ only in the replacement of the C=C groups with N atoms, the ESR spectra of the 5^- species in DMF revealed striking differences with the spectra of 3^-. The $5a^-$ spectrum was simulated using a_H(4 H) = 3.07, a_H(2 H) = 4.24, and a_N(2 N) = 0.76 G. The simulation and assignment of the 4.24-G coupling to the center pair of hydrogens was confirmed from the spectra of $5b^-$ and $5c^-$ which showed a_H(4 H) = 3.19 and a_N(2 N) $\sim$ 0.7 G (Figure 5; Table II). Clearly, the electron density on the bridge is high and much higher than that found for 3^-. Indeed, the $5a^-$ a_H values are quite comparable to those for the anthracene anion radical,[16] for which $a_H = 5.38$ G for the 9,10-hydrogens and 2.66 G for the 1,4,5,8-hydrogens. In a similar light the a_N value for 5^- is smaller than that for 4^-.

High electron density on the bridge makes it unlikely that the electron would be localized on the imide moiety, and the low-temperature spectra confirmed this expectation. Only slight broadening of *all* the lines was evidenced at 210 K. Thus, the ESR data demonstrate that *the odd electron of 5^- is delocalized.* This is in agreement with previously reported optical data.[1]

We have previously discussed the difference in electronic structure of diquinone and diimide anion radicals.[1] Stated concisely, the imide moieties are poorer electron acceptors than quinone units, and therefore, the odd electron will tend to spend more time on the anthracene bridge when it is flanked by imides. This qualitative view is supported by π-MO-PPP calculations on **5**. These calculations show that there are a number of low-lying orbitals for 5^-. Using the calculated SOMO coefficients and the McConnell equation, a_H values were calculated for the various hydrogens of 5^-. As shown in Table II, there was satisfactory agreement between experiment and calculation. Agreement was not achieved for 5^- when a Huckel MO calculation was employed, because a different orbital ordering gave a different SOMO.

Electron Localization and Hopping in 6^-. The ESR spectrum of 6^- taken at 294 K in CH_2Cl_2 (Figure 6) displayed a pentet, $a_N = 1.19$ G, as expected for fast exchange between two equivalent nitrogens. At 210 K this spectrum collapsed to give three broad peaks of equal intensity (Figure 6) with $a_N = 2.34$ G indicative of electron localization. The spectra at intermediate temperatures were simulated to estimate rate constants, and an Eyring plot gave the activation parameters shown in Table III. These values were quite similar to those determined for 3^- and 10^-. Thus, the reorganization energies for electron transfer between imides is

(13) Marcus, R. A. *J. Chem. Phys.* **1956**, *24*, 966.

(14) Fuderer, P.; Gerson, F.; Heinzer, J.; Mazur, S.; Ohya-Nishiguchi, H.; Schroeder, A. H. *J. Am. Chem. Soc.* **1979**, *101*, 2275.

(15) Closs, G. L.; Calcaterra, L. T.; Green, N. J.; Penfield, K. W.; Miller, J. R. *J. Phys. Chem.* **1986**, *90*, 3673.

(16) Bolton, J. R.; Fraenkel, G. K. *J. Chem. Phys.* **1964**, *40*, 3307.

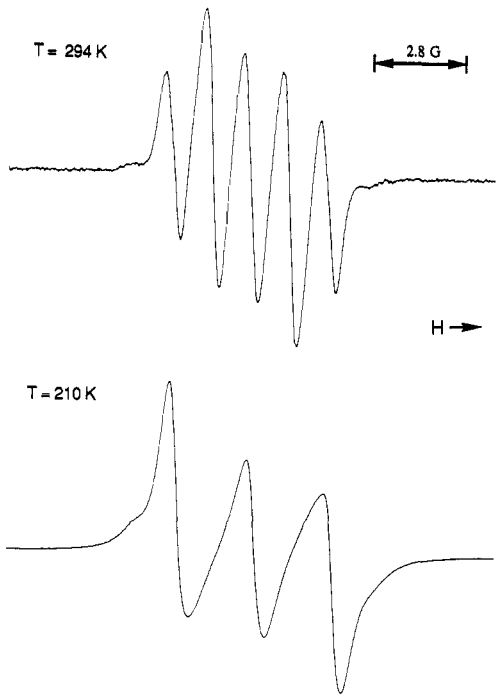

Figure 6. ESR spectra of $\mathbf{6}^-$ in CH_2Cl_2, 0.1 M Bu_4NBF_4, at 294 and 210 K.

quite similar to that for electron transfer between quinones. $\mathbf{6}^-$ was also examined in DMF and gave activation parameters similar to those in CH_2Cl_2. At 340 K in DMF, the spectrum is a 1:2:3:2:1 pentet.

Conclusions. The data make it quite clear that the odd electron on $\mathbf{3}^-$ is localized in an orbital which resembles the SOMO of the naphthoquinone anion radical. It is suggested that localization occurs because these large π-systems are quite polarizable.[3] If the delocalized SOMO has a high electron density on the end electrophores, small distortions of the nuclear framework can make a localized structure more stable than a delocalized one. This localization process will also be favored by solvent organization and ion pairing of cations with the anionic end of the radical anion. The delocalization of $\mathbf{5}^-$ results because its delocalized SOMO has high electron density on the bridge.

It is revealing to compare the properties of $\mathbf{3}^-$ and $\mathbf{10}^-$. The small separation between the first and second reduction potentials reveals a similar isolation of the two electrophores. The electron densities on the quinone units are similarly high, and the rate of electron exchange is quite similar. The similar rate arises because the change in internal modes and solvent modes required for electron transfer is essentially the same for the two ions.

Electron localization in conjugated π-systems is an important problem for materials chemistry and especially for conducting polymers. Most of these polymers are composed of partially oxidized or reduced linear π-systems, and electron localization along these linear systems can be an important factor for conductivity. The individual conducting units, polarons or bipolarons, are solid-state analogues of the ion radicals of interest here. Because these polymers are charged and have counterions, and most contain heteroatoms along the π-system, the possibility of localization is quite real. We have shown how easy it is to localize charge even in small molecules and how small structural changes can convert delocalized to localized structures.

Experimental Section

^1H NMR and ^{13}C NMR were measured using IBM-NR-300-AF (300 MHz) or IBM-IR-200-AF (200 MHz) FT-NMR spectrometers. Chemical shifts are reported in δ units with respect to the $CDCl_3$ protonic impurity peak at 7.257 ppm. Infrared spectra were recorded on a Perkin-Elmer 1600 Fourier transform instrument. Fast atom bombardment (FAB) mass spectra were recorded on a high-resolution VG-7070E-HF instrument. Cyclic voltammograms were recorded on a BAS 100 electrochemical analyzer. Bulk electrolyses were performed with a Princeton Applied Research (Model 173) potentiostat. UV–vis absorption spectra were recorded on a Shimadzu UV-160.

Materials. Anhydrous DMF and CH_2Cl_2 (Aldrich Chemical Co.) were used fresh or after temporary storage over 4-Å sieves. Tetrabutylammonium tetrafluoroborate was recrystallized from H_2O/MeOH, 3:1, and dried in vacuo. 2,3-Dimethyl-1,4-benzoquinone was prepared from 2,3-dimethylphenol.[17] The syntheses of **4**, **5a**, **5b**, and **5c** were described previously.

6,13-Dihexyl-2,3,9,10-tetramethyl-1,4,8,11-pentacenetetrone (3c). 2,3-Dimethyl-1,4-benzoquinone (0.59 g, 4.36 mmol) was dissolved in Decalin (4 mL) in a 50-mL round-bottom flask equipped with an addition funnel, reflux condenser, N_2 inlet, and a magnetic stirring bar. The addition funnel was charged with the benzodifuran precursor **9c** (0.50 g, 0.436 mmol) suspended in Decalin (10 mL). The suspension of **9c** was added to the refluxing quinone solution over a 25-min period. The color changed from yellow to red-brown. After the mixture was refluxed for 30 min, the gray-white precipitate that formed upon cooling was removed by filtration. The filtrate was collected, and the Decalin and unreacted 2,3-dimethyl-1,4-benzoquinone were removed by vacuum distillation. The remaining brown solid was purified by chromatography (silica gel prep plate, CH_2Cl_2 eluent). The material remaining near the origin was collected giving a light brown residue. In the dark, 10 mL of concentrated H_2SO_4 was added to the brown residue. The flask was capped, and stirring was continued for 2 h. The product mixture was poured over crushed ice upon which a dark precipitate formed. The precipitate was collected by filtration, washed with H_2O, and subsequently dried in a vacuum desiccator. A 7-mg portion of the crude solid (121 mg total) was purified by chromatography (silica gel prep plate; CH_2Cl_2 eluent), and the red band (R_f = 0.27) was collected, giving 1.4 mg of the desired product (10% yield). Small amounts of the product were purified in this manner prior to ESR analysis. Initial purification of the crude solid could also be accomplished by sublimation (210 °C, 1 torr). ^1H NMR ($CDCl_3$): δ 9.14 (s, 4 H), 3.76 (m, 4 H), 2.28 (s, 12 H), 1.83 (m, 4 H), 1.63 (m, 4 H), 1.38 (m, 8 H), 0.92 (t, J = 7 Hz, 6 H). ^{13}C NMR ($CDCl_3$): δ 183.94, 145.93, 142.13, 131.52, 128.20, 127.19, 32.59, 31.66, 29.80, 28.86, 22.66, 14.10, 13.41. IR (KBr, cm^{-1}): 2956, 2924, 2858, 1664, 1648, 1610, 1454, 1369, 1283, 1032, 718. HR-FAB-MS (H_2SO_4 matrix) for $C_{28}H_{43}O_4$ ($M + H^+$): calcd 563.3161; found, 563.3138. UV–vis (CH_2Cl_2) (λ, nm (log ϵ)): 526 (4.19), 496 (4.09), 457 (3.87), 428 (3.66), 342 (4.80), 2.61 (4.83).

2,3,9,10-Tetramethyl-1,4,8,11-pentacenetetrone (3b). 2,3-Dimethyl-1,4-benzoquinone (0.57 g, 4.19 mmol) and the benzodifuran precursor **9b** (0.50 g, 0.511 mmol) were added to Decalin (10 mL) in a round-bottom flask equipped with a reflux condenser, N_2 inlet, and magnetic stirring bar. The reaction mixture was heated to 190 °C and allowed to reflux for 3 h. The heating source was removed, and the product mixture was allowed to stand overnight. The precipitate was collected by filtration and washed with hexane (25 mL), CCl_4 (25 mL), $CHCl_3$ (15 mL), and subsequently dried in vacuo. The gray solid was transferred to a round-bottom flask containing 15 mL of concentrated H_2SO_4. The flask was securely fastened to a vortex mixer and allowed to shake in the dark for 3 h. The green H_2SO_4 solution was poured over crushed ice at which point a red/brown precipitate formed. The precipitate was collected by filtration and washed with H_2O. The crude product was triturated twice with $CHCl_3$, giving **3b** as a red powder (170 mg, 84% yield). Additional purification of milligram amounts of **3b** was performed by chromatography (silica gel; $CHCl_3$ eluent; R_f = 0.18). ^1H NMR (C_6D_6/TFA-*d* (5:1)): δ 8.68 (s, 4 H), 8.35 (s, 2 H), 1.80 (s, 12 H). ^{13}C NMR ($CDCl_3$/TFA-*d* (5:1)): δ 185.93, 147.84, 134.21, 133.73, 131.93, 128.69, 13.27. IR (KBr, cm^{-1}): 1662, 1601, 1448, 1374, 1283, 1022, 714. HR-FAB-MS (H_2SO_4 matrix) for $C_{26}H_{19}O_4$ ($M + H^+$): calcd, 395.1283; found, 395.1262. UV–vis ($CHCl_3$) (λ, nm): 491, 464, 335, 253.

Triptycene Bis(4-*tert*-butylphenylphthalimide) 6. The reaction was performed in the dark. *N,N'*-Bis(4-*tert*-butylphenyl)-9,10-dimethoxy-2,3,6,7-anthracenetetracarboxylic acid 2,3:6,7-diimide[1] (17 mg, 2.6×10^{-2} mmol) was suspended in a mixture of $CHCl_3$ (5 mL) and propylene oxide (1 mL) in a round-bottom flask equipped with a reflux condenser, N_2 inlet, and magnetic stirring bar. α-Diazonium chloride benzoic acid (92 mg, 0.50 mmol) was added to the suspension in one portion, and the reaction mixture was heated to 61 °C and refluxed overnight. The heating source was removed, the solvent was evaporated, and the crude product was collected (some starting material remained). Chromatography (silica gel, CH_2Cl_2 eluent) gave a clear oil (R_f = 0.67) that yielded a white precipitate upon addition of 2 mL of cold Et_2O. The sample was cooled in a refrigerator overnight before the precipitate was collected by filtration (6 mg 8.4 μmol, 31%). ^1H NMR ($CDCl_3$): δ 8.18 (s, 4 H), 7.72 (m, 2 H), 7.48 (d, J = 8.6 Hz, 4 H), 7.29–7.19 (m, 6 H), 4.45 (s,

(17) Smith, L. I.; Austin, F. L. *J. Am. Chem. Soc.* **1942**, *64*, 528.

6 H), 1.32 (s, 18 H). IR (KBr, cm^{-1}): 2963, 1777, 1724, 1518, 1376, 1253, 1123, 745. HR-FAB-MS (MNBA matrix) for $C_{46}H_{41}N_2O_6$ (M + H^+): calcd, 717.2965; found, 717.2978.

***endo*-Peroxide 9.** **3c** (0.5 mg) was dissolved in 0.5 mL of $CDCl_3$ in a standard ^1H NMR tube, giving an orange/red solution. The solution was exposed to room light for 15 h during which time the color changed to pale yellow (λ (nm): 324, 267, 224). The ^1H NMR was examined before and after purification by chromatography (silica gel, CH_2Cl_2 eluent), showing that **9** was formed quantitatively. ^1H NMR ($CDCl_3$): δ 8.06 (s, 4 H), 2.80 (m, 4 H), 1.60 (m, 4 H), 1.42 (m, 8 H), 0.95 (m, 6 H). IR (KBr, cm^{-1}): 2956, 2924, 2855, 1660, 1611, 1305, 722. HR-FAB-MS (ONPOE matrix) for $C_{38}H_{43}O_6$ (M + H^+): calcd, 595.3060; found, 595.3074.

ESR Spectra. ESR spectra were recorded on an IBM-Bruker ESP 300 X-band spectrometer equipped with a variable-temperature control unit. The spectroelectrochemical cell consisted of a 8.5-cm-length quartz tube that was constricted to 1.2-mm internal diameter at the bottom. A 7-mm Pt wire was encased with insulation tubing except for an exposed end (ca. 1 cm) which was placed in the constricted portion of the cell. A Pt wire counter electrode and a Ag wire reference electrode were positioned away from the working compartment. Following addition of the sample solution, the cell was sealed with a modified septum and degassed with argon. Reductions were performed by setting the potential slightly positive of the corresponding $E^{\circ\prime}$ values and gradually changing the potential to more negative values. The same ESR tube was used without electrodes present for anion radicals prepared by bulk electrolysis. Temperatures are in Kelvin.

Acknowledgment. P. Kasai and V. Cammarata developed the variable-temperature exchange simulation program. S.F.R. was a DuPont Fellow, 1989-1990. This work was supported by the National Science Foundation.

Uncatalyzed and Chorismate Mutase Catalyzed Claisen Rearrangements of 5,6-Dihydrochorismate and 6-Oxa-5,6-dihydrochorismate

John J. Delany, III, Robert E. Padykula, and Glenn A. Berchtold*

Contribution from the Department of Chemistry, Massachusetts Institute of Technology, Cambridge, Massachusetts 02139. *Received April 5, 1991. Revised Manuscript Received September 27, 1991*

Abstract: The synthesis of 6-oxa-5,6-dihydrochorismic acid (**4**) from D-xylose is described. The half-lives for the uncatalyzed Claisen rearrangements of 5,6-dihydrochorismic acid (**3**) and **4** in D_2O at 30 °C were 49 000 and 1200 h, respectively, compared to a half-life of 15.6 h for chorismic acid (**1**) under similar conditions. Both **3** and **4** were processed by the mutase activity of chorismate mutase–prephenate dehydrogenase from *Escherichia coli* with $k_{cat}/k_{uncat} = 1 \times 10^6$ and 4×10^5, respectively, compared to $k_{cat}/k_{uncat} = 2 \times 10^6$ for **1**.

The rearrangement of chorismate (**1**) to prephenate (**2**) is catalyzed by chorismate mutase. It is the first step in the biosynthesis of phenylalanine and tyrosine from **1**, by what is formally a [3,3] sigmatropic rearrangement, and is one of the most intriguing transformations found in nature (Scheme I).[1] The details of the mechanism of the enzymatic process are not understood irrespective of the extensive investigations from numerous laboratories. In a recent publication, we described studies that defined the structural requirements for catalysis by the mutase site of the biofunctional enzyme chorismate mutase–prephenate dehydrogenase from *Escherichia coli*.[2] Crucial to the study was the demonstration that 5,6-dihydrochorismic acid (**3**, Chart I) was a substrate for chorismate mutase. Described herein are the detailed studies of the thermal and enzyme-catalyzed rearrangement of **3** and the related dihydropyran analogue **4**, which proved to be another effective substrate for chorismate mutase.

Haslam and co-workers reported that **3** did not display any tendency to rearrange with chorismate mutase, but it was a modest inhibitor.[3] The dihydro analogue **3** is, in fact, an excellent substrate for chorismate mutase, but observation of enzymatic catalysis requires special experimental conditions since the uncatalyzed reaction is so slow compared to the uncatalyzed rearrangement of **1**. The dihydro analogue **3** and a 1,2-dihydrochorismic acid of undetermined stereochemistry were prepared by Haslam and co-workers by diimide reduction of (-)-**1**.[3] Selective preparation of the two isomers was accomplished by a clever modification of reaction temperature followed by fractional crystallization. Since we had difficulty with the recrystallization

Scheme I

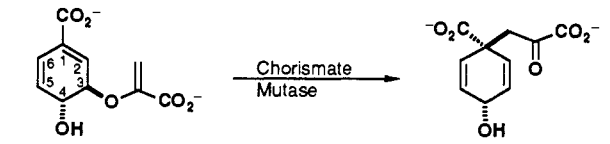

1 2

Scheme II

8 9, X = -NC 10, X = -CN

Chart I

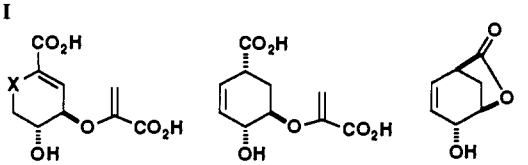

3, X = CH_2 4, X = O 5 6

(1) For reviews, see: (a) Weiss, U.; Edwards, J. M. *The Biosynthesis of Aromatic Compounds*; Wiley: New York, 1980. (b) Haslam, E. *The Shikimate Pathway*; Halstead Press, Wiley: New York, 1974. (c) Ganem, B. *Tetrahedron* **1978**, *34*, 3353-3383.

(2) Pawlak, J. L.; Padykula, R. E.; Kronis, J. D.; Aleksejczyk, R. A.; Berchtold, G. A. *J. Am. Chem. Soc.* **1989**, *111*, 3374-3381.

(3) Ife, R. J.; Ball, L. F.; Lowe, P.; Haslam, E. *J. Chem. Soc., Perkin Trans. 1* **1976**, 1776-1783.

0002-7863/92/1514-1394$03.00/0